Global Change Biology (2002) **8,** 984–998

Simulating fire regimes in human-dominated ecosystems: Iberian Peninsula case study

SERGEY VENEVSKY*, KIRSTEN THONICKE, STEPHEN SITCH and WOLFGANG CRAMER
*Potsdam Institute for Climate Impact Research, Telegrafenberg C4, D-14473 Potsdam, Germany

Abstract

A new fire model is proposed which estimates areas burnt on a macro-scale (10–100 km). It consists of three parts: evaluation of fire danger due to climatic conditions, estimation of the number of fires and the extent of the area burnt. The model can operate on three time steps, daily, monthly and yearly, and interacts with a Dynamic Global Vegetation Model (DGVM), thereby providing an important forcing for natural competition. Fire danger is related to number of dry days and amplitude of daily temperature during these days. The number of fires during fire days varies with human population density. Areas burnt are calculated based on average wind speed, available fuel and fire duration. The model has been incorporated into the Lund-Potsdam-Jena Dynamic Global Vegetation Model (LPJ-DGVM) and has been tested for peninsular Spain. LPJ-DGVM was modified to allow bi-directional feedback between fire disturbance and vegetation dynamics. The number of fires and areas burnt were simulated for the period 1974–94 and compared against observations. The model produced realistic results, which are well correlated, both spatially and temporally, with the fire statistics. Therefore, a relatively simple mechanistic fire model can be used to reproduce fire regime patterns in human-dominated ecosystems over a large region and a long time period.

Keywords: areas burnt, coarse-scale modelling, fire model, human-caused fires, number of fires, Spain

Received 13 November 2001; revised version received and accepted 19 March 2002

Introduction

Fires have a large impact on vegetation and ecosystem structure. By killing vegetation, fires open closed canopies and facilitate seed germination for certain species, thereby influencing both the seed pools and vegetative propagules in the soil. Fire is important in the life cycle of many plant species and for their competitive abilities, thereby contributing to the structure of plant communities. Associated with fire is a release of carbon into the atmosphere. On the global scale, the total biomass burnt is about 4.5 Pg C $year^{-1}$, of which more than 2.5 Pg C $year^{-1}$ are released in savannah and forest ecosystems (Levine, 1996). This value is comparable to other major fluxes in the global carbon budget (5.5 Pg C $year^{-1}$ for industrial emissions, about 2 Pg C $year^{-1}$ ocean uptake, 1.5 Pg C $year^{-1}$ land use) (IPCC, 1995). Therefore, fire is an integral part not only in vegetation succession, but also in global biogeochemical cycles.

Correspondence: Sergey Venevsky, tel. + 49 331 288 2606, fax + 49 331 288 2600, e-mail: sergey.venevski@pik-potsdam.de

A variety of models (see review in Gardner *et al*., 1999) have been developed to describe fire effects in natural ecosystems. Statistical fire models (e.g. Johnson & Gutsell, 1994), using Weibull probability distributions as a function of stand age imply a static fire regime. Application of such concepts to new environmental conditions (i.e. another study region or changed climatic conditions at the site) would require new parameterisations. An analysis of the ecosystem component responsible for changes in a particular fire regime cannot be identified using this modelling approach. To study various facets of the vegetation–fire interaction, an explicit simulation of fire dynamics (fire ignition and spread conditions) and its effects on vegetation regeneration (fire intensity, area burnt and subsequent successional dynamics) is required. Such a mechanistic modelling approach would allow studies under changing environmental conditions. Physical models (Rothermel, 1972; Albini, 1976), later adapted to Chaparral ecosystems by Davis & Burrows (1994), simulate fire dynamics explicitly and can be applied at small scales (hectares to square kilometres). To model fire dynamics at scales of coarse-scale vegetation

dynamics (i.e. at a spatial resolution of 100–10 000 km^2 and at daily to annual time steps, but applied over an investigation period of several decades), a generalization of this concept as well as its parameterisations are required.

Different generalizations have been made regarding scaling and in modelling fire dynamics, and its effects on vegetation dynamics. These studies differ in their interpretation of process relevance at coarser scales. Lenihan & Neilson, 1998) uses a combination of physical models to describe fire occurrence and spread in the model MCFIRE. Keane (1996b) uses Weibull probability distributions in FIRE-BGC for fire ignitions. Fire behavior and spread is then explicitly modelled using physical models FARSITE (Finney, 1994). This approach fixes the fire weather conditions causing fire ignition to the historical pattern and therefore ignores any changes in the fire weather system. Consideration of human and natural ignition sources, such as in CRBSUM (Keane *et al*., 1996a) in which probability functions are used, can be used as a tool for fire management and land use strategies. Thus, a fire weather index, interpreting the fire danger in certain climatic conditions, combined with a rather mechanistic formulation of human-caused ignitions would be the preferable tool to model fire occurrence. This would allow a more realistic representation, since in some ecosystems 85–97% of the fires are human-caused (Moreno *et al*., 1998; Shvidenko *et al*., 1998). The need for improved coarse-scale fire models, which can also be used for practical fire management, has been identified by Keane & Long (1998). The successional pathway approach to model post-fire succession at the coarse-scale in CRBSUM, does not consider new successional dynamics, which could develop in a changing environment. This can be done using a vegetation model, which simulates vegetation processes dynamically.

The main problems simulating coarse-scale fires at the regional scale were described by McKenzie *et al*. (1996) as follows:

- A lack of data on the ecological effects of fire at coarse spatial resolution complicates model development and validation.
- Process-based fire models were built for fine scales (from hectares to square kilometres) and thereby assume ecosystem homogeneity, which is no longer the case at regional scales.
- Landscape patterns influence both ignition and fire spread; however, these patterns are poorly (if at all) described on a coarse scale.

The importance of specific fire-relevant processes depends on the spatial and temporal scale, which needs to be recognized when their functional representation in fire models is applied at a different scale. Therefore, generalizations of the model concept, re-parameterisation and validation of the modelled processes become necessary.

In order to improve our understanding of fire regimes and their effects on vegetation dynamics, and considering the new requirements, we have developed the model Reg-FIRM (Regional FIRe Model). This model simulates general fire dynamics based on physical models and explicitly considers different ignition sources. It is designed for fire simulation at coarse spatial scales (100–2500 km^2) and can be adapted for calculation on daily, monthly or yearly time steps.

The Reg-FIRM is designed as a further development of our previous fire model Glob-FIRM (Thonicke *et al*., 2001), which combines the fire history concept (Johnson & Gutsell, 1994) with process-orientated fire modelling. Glob-FIRM simulates fire regimes at the global scale and coarse-scale fire–vegetation interactions.

We incorporated Reg-FIRM into the Lund-Potsdam-Jena Dynamic Global Vegetation Model (LPJ-DGVM, Sitch *et al*., 2002) to allow dynamic interactions between fire and vegetation. Reg-FIRM provides area burnt for the DGVM by estimating the number of fires, which depends on climatic fire danger, both human and natural-caused ignitions, and the average size of a fire in a grid cell.

In this study the regional fire model Reg-FIRM was run inside the LPJ-DGVM at a daily and monthly time step for the period 1974–94 at a spatial resolution of $0.5° \times 0.5$ longitude/latitude across the Iberian Peninsula, as an example of a fire-prone ecosystem with dominance of human-caused fires. Using this tool we want to study the role of the different fire drivers on the spatial and temporal pattern of fire. Here, we show that a simple non-statistical formulation can integrate the various reasons for human-caused fires. This approach, a generalization of physical models to describe fire spread is sufficient to reproduce the observed pattern at the regional scale.

Methods

Fire effects are a product of fire ignitions, number of fires, fuel characteristics and the persistence of positive burning conditions over space and time, resulting in fire spread during a certain fire duration, and certain area burnt. Post-fire conditions then determine vegetation regeneration, which feeds back on the fire-driving conditions through new fuel development and species flammability. By separately calculating number of fires and area burnt, the model allows a direct comparison to the available fire statistics. The

following equation is the basis of the regional-scale fire model:

$$PB(t) = \frac{\sum_{N_{\text{fire}}(t)} S_{N_{\text{fire}}}(d_N)}{S_{\text{grid}}} \quad (1)$$

where $PB(t)$ is the fraction of a grid cell burnt up to time t (between zero and one), $N_{\text{fire}}(t)$ is the number of fires in the period $(0, t)$, $S_{N\text{fire}}$ is the area burnt by the fire number N, d_N is the duration of this fire and S_{grid} is the area of a grid cell. In the following section, the design of the model components will be described in detail.

This model concept implies that within one time step fires burn with the same characteristics and have an equal impact on the final area burnt. Additionally, the applicability of the equation is limited by the lowest value of S_{grid}, which should not be less than 100 km^2. Otherwise, the complete grid cell would burn and fire spread to neighbouring cells would have to be incorporated into the model. Therefore, the equation does not describe extremely large convective fires, but considers rather average fire conditions. These relatively rare events may be described using special statistical and physical methods reviewed elsewhere (Valendik *et al.*, 1978; Moritz, 1997).

Equation 1 can be applied in three modes, with a daily, monthly or yearly time step. Implementing the equation with a daily time step assumes stochastic ignition, duration of fire and application of fine-scale physical models of fire spread (Van Wagner, 1969; Rothermel, 1972; Albini, 1976). By integrating fire behavior and fire effects over a simulation year, one obtains the annual area burnt, which corresponds to the fire regime of a grid cell. The fire regime for a grid cell can also be assessed annually, although less accurately, using mean annual values of number of fires and mean area burnt if we assume that all the fires during the year have an equal impact. This approach is less computationally expensive (for instance, by excluding daily weather simulation) and also enables one to obtain the response of the fire regime to climate driving forces on a monthly and yearly time step.

Implementation

We assume that at the regional scale fire disturbance in an ecosystem can be described by the following processes: occurrence of fire danger associated with dry weather; fire ignition, possibly affected by human activity; fire spread, forced by available fuel and wind; fire termination due to weather or suppression activities; and fire-induced vegetation mortality (see, e.g. Whelan, 1995). With a total fuel load of less than 200 gC m^{-2} no ignition and fire spread is possible (see Thonicke *et al.*, 2001).

Fire danger

Since most fires are initiated in the litter layer, a series of models are required to simulate wetting and drying processes in the ground fuel layer during changing weather conditions. Several fire rating systems have been proposed which estimate the ignition potential of fuel, mainly as variations of the Canadian Forest Fire Weather Index (Van Wagner 1987), the American National Fire-Danger Rating System (Deeming *et al.*, 1974) or the Nesterov Index which is widely used in Russia (Nesterov, 1949).

We use the Nesterov Index (NI) for the fire danger rating mainly because it is a relatively simple equation and does not require variables such as daily wind speed or daily humidity, for which accurate data are practically unobtainable over large regions. A comparison of Canadian and Russian fire danger systems with the satellite measurements in 1992 for Central and Eastern Siberia shows that both rating systems successfully tracked the increasingly extreme fire danger condition (Stocks *et al.*, 1996). The Nesterov Index, however, is the only suitable one for estimation of ignition potential in comparison with the other two rather complex fire rating systems, because it drops to zero rapidly after a small amount of rain.

The Nesterov Index was derived as an empirical function reflecting the relationship between fire and weather based on historical data (Nesterov, 1949). It is calculated using daily temperature (at 15 h), dew-point temperature, and precipitation. The difference between the two temperatures is multiplied by the daily temperature and summed over the number of days since the first day, in which precipitation dropped below 3 mm:

$$NI(N_d) = \sum_{if\ P(d)\le 3mm}^{N_d} T_{\text{daily}}(d) * (T_{\text{daily}}(d) - T_{\text{dew}}(d)) \quad (2)$$

where $NI(N_d)$ is the Nesterov Index ($^\circ\text{C}^2$)for day N_d, and d is a positive temperature day with a precipitation of less than 3 mm. When the daily precipitation exceeds 3 mm, the Nesterov index falls to zero. *NI* values between 300 and 1000 are considered to be moderate for ignition potential. *NI* values ranging between 1000 and 4000 represent high ignition potential, while values above 4000 represents extreme potential for ignition.

The following equation is a discrete approximation of the *NI*:

$$NI(N_d) = \sum_{if\ S\le m_e}^{N_d} \frac{(T_{\max}(d) + T_{\min}(d))}{2} * \left[\frac{(T_{\max}(d) + T_{\min}(d))}{2} - (T_{\min}(d) - 4)\right] \quad (3)$$

where the summation is made over the dry days with a positive minimum daily temperature and when the relative soil moisture $S(d)$ in the upper soil layer, expressed in relative volumetric units, is less than the moisture of extinction m_e, above which fire can not spread (Albini, 1976). In the model, a value of 0.3 for woody and 0.2 for herbaceous vegetation types is taken for m_e (Thonicke *et al.*, 2001). $T_{\min}(d)$ and $T_{\max}(d)$ are daily minimal and maximal temperatures, while ($T_{\min}(d)$-4.0) represents a simple approximation of $T_{\text{dew}}(d)$, the daily dew point temperature (Running *et al.*, 1987).

Expressing equation 3 as a continuous function we obtain on a daily time step:

$$NI(N_d) = \int_0^{N_d} f(S(t)) * \left[\frac{\left(T_{\max}(t)^2 - T_{\min}(t)^2\right)}{4} + 2*(T_{\max}(t) + T_{\min}(t))dt \right] \quad (4)$$

where $f(S(t)) = \exp\left(-\pi * \left(\frac{S(t)}{m_e}\right)^2\right)$ is a simple probability function for a dry day. Estimates of NI at monthly and yearly simulation time steps are based on monthly or seasonal averages of $T_{\min}(d)$ and $T_{\max}(d)$:

$$NI_m = \left(\frac{\left(T^m_{\max}{}^2 - T^m_{\max}\right)^2}{4} + 2 * \left(T^m_{\max} + T^m_{\min}\right) \right) * \int_0^{N^m_d} f(S(t))\mathrm{d}t \quad (5)$$

and

$$NI_S = \left(\frac{\left(T^S_{\max}{}^2 - T^S_{\min}{}^2\right)}{4} + 2 * \left(T^S_{\max} + T^S_{\min}\right) \right) * \int_0^{N^S_d} f(S(t))\mathrm{d}t \quad (6)$$

where NI_m represents the accumulated Nesterov Index for month m (with positive minimum daily temperatures), assuming minimal and maximal temperatures $T^{\mathrm{m}}_{\max}$ and $T^{\mathrm{m}}_{\min}$ are constant during the month and equal to their mean values. N^m_d is the total number of days in month m. The integral over $f(S(t))dt$ for the time N^{m}_d describes the season of critical fire conditions in the fuel bed and is named hereafter as the length of the fire season. NI_s is the accumulated Nesterov Index for an entire season with positive minimal daily temperatures, and $T^S_{\max}$, $T^S_{\min}$ are averaged over this period. N^S_d is number of days with positive minimum daily temperatures in a year.

The fire danger index *FDI*, based on the Nesterov Index, should interpret qualitative risk terms such as low, moderate, high and extreme ignition potential in quantitative terms. A smooth risk probability function for fire danger with a daily time step is

$$FDI(N_d) = 1 - \exp(-\alpha * NI(N_d)) \quad (7)$$

while for average monthly and annual values of FDI we receive

$$FDI(m) = \frac{1}{NI_m} \int_0^{NI_m} (1 - \exp(-\alpha * NI))d(NI) = 1 + \frac{1}{\alpha * NI_m} * (\exp(-\alpha * NI_m) - 1) \quad (8)$$

and

$$FDI(s) = 1 + \frac{1}{\alpha * NI_s} * (\exp(-\alpha * NI_s) - 1) \quad (9)$$

respectively.

The tuning parameter α ($^\circ\mathrm{C}^{-2}$) can be used to provide different values of probability for low, moderate, high and extreme ignition risks, based on NI values. It is set at 0.000337 resulting in upper limits for daily *FDI* of approximately 0.1 for low, 0.3 for moderate, 0.75 for high and 1 for extreme ignition potentials according to (9). It can be redefined when detailed observations are available.

Number of fires

Nowadays, human-caused fires dominate over fires induced by lightning in many natural ecosystems, e.g. lightning-caused fires accounted for only 3% of the fires that occurred in Spain between 1974 and 1994 (Moreno *et al.*, 1998). Even the more remote regions have a larger number of human-induced fires than lightning-caused. For example, lightning caused only 13.7% of the fires in the boreal zone of Russia between 1986 and 1995 (Shvidenko *et al.*, 1998).

A simple estimate of the number of lightning-caused fires l per area and day of fire season can be derived from the total number of lightning-caused fires during 20 years in Spain (5663 (Moreno *et al.*, 1998) within a total area of 505 10^3 km^2, assuming a season length with fire danger equal to 200 days (Melekhov, 1978; Korovin, 1996). The derived value of l, equal to 0.028 of lightning fires per day per million hectares is similar to a value of 0.015 for the boreal zone of Russia (Telitsyn, 1988). We took a value of $l = 0.02$ as a constant rate for this version of Reg-FIRM.

Ignition sources related to human activity are rather different. The majority are related either with recreation or labour activities of humans, the remaining related to intentional clearing of vegetation (Goldammer & Jenkins, 1990). Generally, human-caused fires are concentrated near human settlements or transportation routes, i.e. are related to the spatial distribution of human population and the accessibility of natural ecosystems (see Pausas & Vallejo, 1999; for the case of Iberian Peninsula). On the other hand, human ignition potential depends on economic status and life style. With growth of urban population, people tend to spend more labour and recreation time within cities. Therefore, human-caused ignitions are hypothesized to be dependent on the population density to which various life styles are assigned as a simple approximation.

The following simple composite function describes the total daily number of possible ignition causes, human and natural, for a grid cell:

$$N_{ig}(N_d) = (k(P_D) * P_D * a(N_d) + l) * S_{\text{grid}} \qquad (10)$$

where N_{ig} is the total number of ignitions for a day N_d in a grid cell, P_D is the population density per km^2 in a grid cell, S_{grid} is the area of a grid cell in million ha. $k(\mathrm{P}_D)$ is a scaling function representing different ignition potentials of humans in densely populated and scarcely populated regions due to differences in spatial patterns of human settlements and the exposure of humans to natural ecosystems. We took the known function of fire danger, in terms of population density representing exposure of humans to natural ecosystems, following Telitsyn (1988), and expressed in relative units:

$$k(P_D) = 6.8 * P_D^{-0.57} \qquad (11)$$

The function implies that an average person in scarcely populated regions like Australia, Canada or Russian Asia potentially produces three to four times more ignitions (because of longer activities within natural ecosystems) than, for example, an average person in densely populated regions of Europe.

Human ignition potentials

The stochastic variable $a(N_d)$ is the number of ignitions produced by one human during day N_d multiplied by a factor 10^4 (in order to scale the population density per million ha). We assume that this stochastic variable is distributed exponentially (i.e. a probability density function for $a(N_d)$ is λ*exp$\langle -\lambda a\rangle$). The mathematical expectation $(1/\lambda)$ of this distribution depends on life style and wealth status of humans. For example, a value $1/\lambda = 0.1$ is obtained using the annual average number of fires during the period 1980–89 for northern circumpolar countries together with their human population (Stocks 1991). The mathematical expectation has the physical meaning that almost one out of ten humans produce one ignition in a natural ecosystem during the person's active labour and/or leisure lifetime (30 years). Such a rather heuristic hypothesis results, for example, in 0.25 ignitions in a day per one million hectares for regions with a population density of two persons per km^2, which is in agreement with the value observed for northern regions of the Russian Far East with the same population density (Shvidenko *et al.*, 1998). For peninsular Spain the value $1/\lambda = 0.22$ is obtained from the number of human-caused fires (pasture burning, caused by negligence or intentional) during the period 1974–94 (Moreno *et al.*, 1998; Table 6) and the average human population density over the region. The uniformly distributed random number p_d used to calculate the value of $a(N_d)$ is given by:

$$a(N_d) = -\frac{\ln p_d}{\lambda} \qquad (12)$$

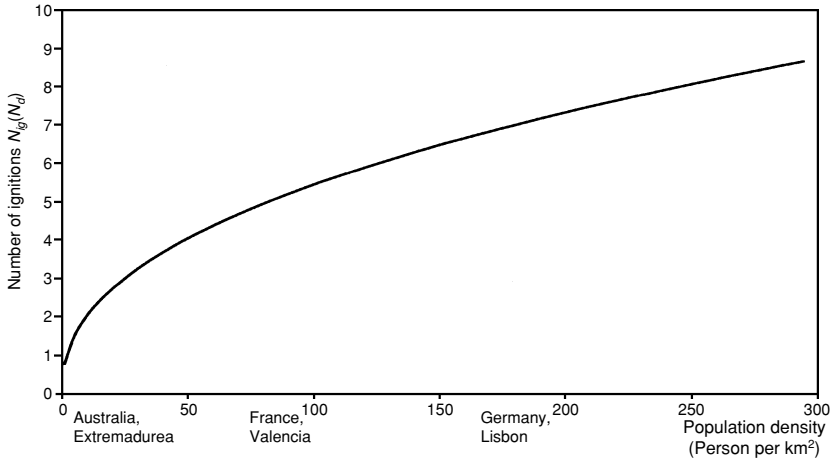

Fig. 1 Number of possible ignitions for a day per million ha $N_{ig}(N_d)$ related to human population density.

where $\lambda = 1/0.22$. Figure 1 illustrates the number of ignitions following equation 10.

Therefore, the annual average number of fires $N_{\text{fire}}(s)$ for a grid cell can be estimated as:

$$N_{\text{fire}}(s) = FDI(s) \int_{\text{When } T_{\min} \geq 0} f(S(t))\mathrm{d}t * \left(\gamma * P_D^{\Theta} + l\right) * S_{\text{grid}}, \quad (13)$$

where γ is a constant equal to 1.496 and Θ is equal to 0.43 for peninsular Spain (see 10, 11 and 12). The number of fires in a month can be calculated in the same way as the annual calculation (see 11–13).

Equation 13 has almost the same mathematical formulation as the equation used by the Russian forestry practice to estimate the annual number of fires per million hectares over large administrative units:

$$N_{\text{fire}}(s) = C(s) * N_d(s) * \left(\delta * P_D^{0.5} + l\right) \quad (14)$$

where *C(s)* is a fire danger coefficient, based on the Nesterov Index, N_d(s) is the number of days with moderate, high and extreme fire danger, estimated using the Nesterov Index, and δ is a coefficient of population fire activity for a region (Melekhov, 1978). However, estimates of C(s), $N_d(s)$ and δ can be rather complex in this method. Therefore, equation 13 with the underlying approximations is used in the model concept.

Humans tend to have different motivations to ignite fires, reflecting regional differences in their socioeconomic background. These need to be taken into account, when estimating human ignition potentials for a given region. Examples of regional variation are presented below. Ranges for the constants Θ and γ (and a(N_d)) can be estimated for a region, given the other variables in equations 1 and 13 are known *apriori* or can be assumed, and a distribution of area burnt by population density classes is identified. The values of constants will be estimated for Africa to prove the validity of the approach for all regions. This is done using the mean percentage of area burned in each population class relative to the total extension of the class itself for the period 1985–91 (see Table 10 in Barbosa *et al*., 1999).

Indeed, the mean annual percentage of area burned PB_{mean} by population density can be approximated as (see 1,13):

$$PB_{\text{mean}} = FDI_{\text{mean}} \int_{\text{When } T_{\text{mean}} \geq 0} \tilde{f}(S(t))\mathrm{d}t * \left(\gamma * P_D^{\Theta} + l\right) * \tilde{S}_{\text{fire}} \quad (15)$$

where FDI_{mean} is mean value of the fire danger index, $\int_{\text{when } T_{\text{mean}} \geq 0} \tilde{f}(S(t))\mathrm{d}t$ is the average length of fire season, $\tilde{S}_{\text{fire}}$ is the average fire size in million hectare. For Africa FDI_{mean} is set to one, the average length of fire season $\int_{\text{when } T_{\text{mean}} \geq 0} \tilde{f}(S(t))\mathrm{d}t$ to 182 days (half a year, see Barbosa *et al*., 1999), and lightning fires ($l = 0$) are neglected. From these variables, the average fire size for Africa is the most uncertain, since long-term observations are missing. For example, for Kenya the average fire size varies from 347 ha in 1990 to 40 ha in 1999 (Ndambiri & Kahuki, 2001). Therefore, average fire size $\tilde{S}_{\text{fire}}$ is set to $150{*}10^{-6}$ million ha, which is the average value for shrublands according to Keane & Long (1998).

The values for Θ and γ (and a(N_d)) are calculated through logarithmic regression of PB_{mean} by P_D. PB_{mean} was obtained from satellite observations, where two methods, Sc1 and Sc2, were used to detect area burnt (Barbosa *et al*., 1999). The first method (Sc1) is believed to overestimate the total area burned, while the second (Sc2) is probably near to the minimum value for burned area estimations. The values of Θ and γ (and a(N_d)), obtained for the Sc2 method, are close to those used for peninsular Spain: $\Theta = 0.4$; , $\gamma = 1.93$ and a(N_d) = 0.28. For the Sc1 method these values are equal to $\Theta = 0.4$, $\gamma = 3.43$ and a(N_d) = 0.51. Therefore, the exponent Θ, describing the spatial distribution of human settlements in relation to fires, does not vary much by geographical region (see also equation 14). On the other hand, the number of ignitions produced by one human during the day, a (N_d), can differ several times, depending on life style (rural vs. urban, traditional vs. modernized) and land use practices among regions.

Fire spread

Active fires increase in size depending on their rate of spread, as the flame front moves through the fuel bed and favourable burning conditions continue over time (defined as the duration of a fire). The rate of spread is driven by wind and fuel characteristics. The more energy the flame front can build up, the faster the fire can spread. The combined influence of these factors results in a specific geometric shape, the fire perimeter, from which the area burnt can be deduced. The impact of topography, another important driving factor, is not considered at this stage.

Here, the fire spread model on a daily time step is based on the hypothesis that we can not distinguish between different burning conditions of each fire in a grid cell and the assumption, that all fires, started in one day, have the same (stochastic) duration and (constant) rate of spread:

$$PF(N_d) = \pi * U(N_d) * d(N_d). \quad (16)$$

$PF(N_d)$ is the perimeter of the fire, $U(N_{\text{d}})$ is the frontal fire rate of spread, $d(N_d)$ is a stochastic duration of fire initiated in a day N_d. This method generalizes fire-spread functions for single fire events to the application at the

regional scale. Within one day the probability that within one grid cell (note the cell size chosen at the regional scale) burning conditions are notably different between each fire, is very low. We used an exponential distribution for the duration of fire (the probability density function being $\mu*\exp(-\mu d)$), with a mathematical expectation approximately equal to one day (1.0). This distribution function provides a good fit to the histogram for duration of fire incidents, based on 50 year fire statistics for Russia (Korovin, 1996). Values for $d(N_d)$ are obtained from equation 12 with $\lambda = \mu = 1/1.0$

Rate of spread $U(N_d)$ is estimated using the Rothermel (1972) approach to fire spread modelling, but in a rather simplified form, as proposed by Telitsyn (1988, 1996):

$$U(N_d) = U_0(N_d) * \left(1 + A * W(N_d)^B\right) \tag{17}$$

where $U_0(N_d)$ is the rate of spread for the backing fire (i.e. without wind) in m s^{-1}, $W(N_d)$ is the wind speed in m s^{-1}, A and B are constants (Rothermel, 1972). We fixed both the constants A and B to 1.0, according to Telitsyn's (1996) approximation, and do not simulate wind speed, assuming an average value of 3.7 m/s according to Vázquez & Moreno (1998). The constant value of wind speed was taken because of the general absence of a coarse-scale wind model with daily resolution.

The rate of spread for a backing fire was approximated by Telitsyn (1988, 1996) from heat balance equations for inward burning within the fuel bed:

$$\sigma * E_i * \left(T_f^4 - T_0^4\right) = \rho(N_d) * [c(t_i - t_0) + L * \omega(N_d)] * U_0(N_d) \tag{18}$$

where σ is the Stefan-Boltzman constant $5.7*10^{-8}$ J m^{-2} K^{-4} s^{-1}, E_i is the inward emissivity of the 'flame-fuel' system. T_f and T_0 are the absolute temperatures of the flames and fuel surface in K, respectively. $\rho(N_d)$ is the bulk density of the fuel bed in kg m^{-3}, c is specific heat of fuel in J kg^{-1} C^{-1} and t_i is the ignition temperature of fuel in °C. t_0 is the temperature of fuel surface in °C, L is the latent heat of evaporation $2.6\ 10^6$ J kg^{-1} and $\omega(N_d)$ the fuel moisture content expressed as a mass fraction.

Assuming that some of the parameters are constant, as given in published data (Davis et al., 1959; Rothermel, 1972; Demidov & Saushev, 1975), we obtain the following approximation for $U_0(N_d)$

$$U_0(N_d) = \frac{3 * E_i}{\rho(N_d) * (16 + \omega(N_d) * 100)} \tag{19}$$

when $T_f = 1200$ K, $T_0 = 293$ K, $C_i = 1400$ J/kg C^{-1}, $t_i = 300$ °C, $t_0 = 20$ °C (Telitsyn, 1996).

We take the soil moisture $S(t)$ in the upper 50 cm of the soil as a surrogate for the fuel moisture content and $\rho(N_d)$ as the fuel bulk density, weighted by local vegetation types:

$$U_0(N_d) = \frac{3 * E_i}{\sum_j w(j)\rho_j(N_d) * (16 + S(N_d) * 100)} \tag{20}$$

where $w(j)$ is the fractional ratio of a given vegetation type j at the location. Since fuel bulk densities differ between vegetation types j, fuel flammability will vary according to vegetation composition.

The inward emissivity of the 'flame-fuel' system E_i varies for low-intensity fires between 0.1 and 0.3, and between 0.3 and 0.7 for fires of moderate intensity (Thomas, 1965; Demidov & Saushev, 1975; Telitsyn, 1996).

The perimeter shape of a wind-driven fire can often be approximated by an ellipse (Van Wagner, 1969). According to this approximation the ellipse will have an elongated semi-major axis in the wind direction and the smaller axis represents the progress of the backing fire (Albini, 1976). Complex exponential regression equations for parameters of elliptical models for areas burnt by wind speed were elaborated at the Northern Forest Fire Laboratory, Missoula, USA (see Albini, 1976). An application of these equations within a range of wind speeds between 0 and 4 m/s results in a ratio of semi-major to semi-minor axes for an elongated ellipse of between 0.45 and 0.6; a value of 0.5 for a wind speed of 3.7 m/s. This two-to-one relation between the length and width of area burnt is often observed for fires in the boreal zone (Melekhov, 1978). It allows us to make simple estimates of area burnt assuming that it is approximately one half the area of a circle with a diameter equal to the elongated axis of the downwind driven ellipse:

$$S_{\text{fire}} = 0.5 * \frac{PF^2(N_d)}{4 * \pi} \tag{21}$$

A simplified version of the last equation ($S_{\text{fire}} = 0.04*PF^2$) is applied for practical purposes by the Russian Forest Service to obtain a rough estimate of fire spread (Far Eastern Forest Institute, 1987).

The average annual fraction burnt is relatively straightforward to derive, if one assumes that fuel physical parameters are constant (i.e. average rate of spread $\overline{U}$ is constant) during a year (see 1, 13, 6 and 20):

$$PB(s) = \frac{N_{\text{fire}}(s) * \pi * \overline{U}^2}{8 * S_{\text{grid}} * \mu^2} \tag{22}$$

The monthly fraction burnt can be calculated in the same way.

The Lund-Potsdam-Jena Dynamic Global Vegetation Model

Reg-FIRM was incorporated into the Lund-Potsdam-Jena Dynamic Global Vegetation Model (LPJ-DGVM, Sitch *et al*., 2002) and tested over peninsular Spain for the period 1974–94. The vegetation processes relevant to fire, in terms of driving fire and fire effects, will be described in the following section.

The LPJ-DGVM was constructed in a modular framework. Individual modules describe key ecosystem processes, including vegetation establishment, resource competition, growth and mortality. Vegetation structure and composition is described by nine plant functional types (PFTs), which are distinguished according to their plant physiological (C_3, C_4 photosynthesis), phenological (deciduous, evergreen) and physiognomic (tree, grass) attributes. Other land cover types, including agriculture and pastures, and the historical impacts of land-use on vegetation dynamics are not considered here. The model is run on a grid cell basis with input of soil texture, monthly fields of temperature, precipitation and percentage sunshine hours. Each grid cell is divided into fractions covered by the PFTs and bare ground. The presence and fractional coverage of an individual PFT depends on its specific environmental limits, and on the outcome of resource competition with the other PFTs. The annual values of foliar projective cover of PFTs in a grid cell were used as the fractional ratios of different vegetation types $\omega(j)$ in order to estimate average rate of fire spread in the fire model (see equation 20).

The two-layer soil water balance model is based on Haxeltine & Prentice, 1996. Moisture in each layer, expressed as a fraction of water holding capacity $S(N_d)$, is updated daily. Percolation from the upper to the lower layer, and absolute water holding capacity are soil texture dependent. The value of $S(N_d)$, used in the fire model (see equations 13, 19), is also affected by the water use efficiency of the vegetation in the LPJ-DGVM. Extensive water use by a PFT can increase the fire risk by lowering soil moisture content.

Establishment and mortality are modelled on an annual basis. Plant establishment, in terms of additional PFT individuals, depends on the fraction of bare ground available for seedlings to successfully establish. Natural mortality is taken as a function of PFT vigour, and corresponds to an annual reduction in the number of PFT individuals. Dead biomass enters one litter pool and two soil pools. Mortality also occurs due to fire since the areas occupied in a grid cell by each PFT decreases proportionally to the total area burnt. The number of individuals surviving a fire is defined for each PFT (expressed in terms of a fraction, see Thonicke *et al*., 2001). Vegetation types are therefore differentially affected by fire. The bare ground opened by fire is used for establishment of seedlings, providing a feedback between fire and vegetation in the LPJ-DGVM.

Data

Parameters of the fire model

The number of ignitions produced by one human a(N_d) was set to 0.22 and fire duration $d(N_d)$ to 1.0. The inward emissivity of the 'flame-fuel' system E_i was fixed at 0.3, assuming that fires had moderate intensity in peninsular Spain during the simulation period. Fuel bulk densities of the four PFTs occurring in the Iberian Peninsula as defined by the LPJ-DGVM, are listed in Table 1.

Model input

All input data sets were provided at a $0.5^\circ \times 0.5$-longitude/latitude spatial resolutions. The monthly climate data (precipitation and temperature) were provided by the CCMLP project (Carbon Cycle Model Linkage Project) over the historical period 1860–1995 and derived from the data of Hulme (1995) and Jones (1994). Historical CO_2 concentrations were derived from ice core and atmospheric measurements (Enting *et al*., 1994). Soil texture information was obtained from the

Table 1 Fuel bulk density by Plant Functional Type (PFT) used in LPJ-DGVM. The values were obtained from the table of fuel parameters for the Mediterranean region used by the Spanish Environmental Ministry (Ministerio de Medio Ambiente, España) for fire management (Merida, 1999). The 13 fuel types in this table were combined into the five appropriate PFTs of the model. PFT specific fuel bulk density was calculated dividing the average fuel load by the average fuel depth

Plant functional types	Fuel bulk density (kg m^{-3})
Temperate needle-leaved evergreen tree (e.g. Abies alba, *Pinus sylvestris, P. nigra, P. halepensis*)	16
Temperate broadleaved evergreen tree (e.g. *Quercus ilex*, *Qu. suber, Qu. coccifera*)	10
Temperate broadleaved summergreen tree (e.g. *Fagus silvatica, Quercus robur, Castania* spp., *Betula* spp.)	10
C3 perennial grass (graminoids)	2
C4 perennial grass	2

FAO soil data set (FAO, 1991). Population density data from 1990 onwards were extracted from the global population density at a 5′ resolution and up-scaled to a 0.5° grid (Zobler, 1986; FAO, 1991). The population growth rate for the period 1974–94 was obtained from the Spanish National Institute of Statistics (Instituto National de Estadistica, 1999).

The model was validated by comparing simulation output with published data of number of fires and area burnt in peninsular Spain during the period 1974–94 (Moreno *et al.*, 1998). These data include the geographical distributions of number of fires and areas burnt for the entire period and their yearly course.

Results

Geographical distribution

The simulated geographical distribution of number of fires and area burnt over peninsular Spain during the period 1974–94 generally reproduce the observations (compare Figs 2 and 3 with Fig. 4 in Moreno *et al.*,

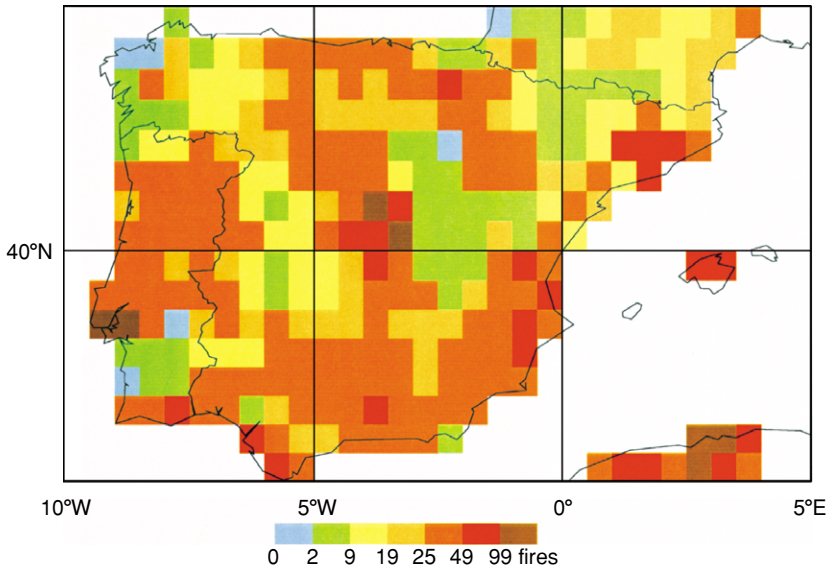

Fig. 2 Simulated number of fires per 100 km^2 on the Iberian peninsula during 1974–94.

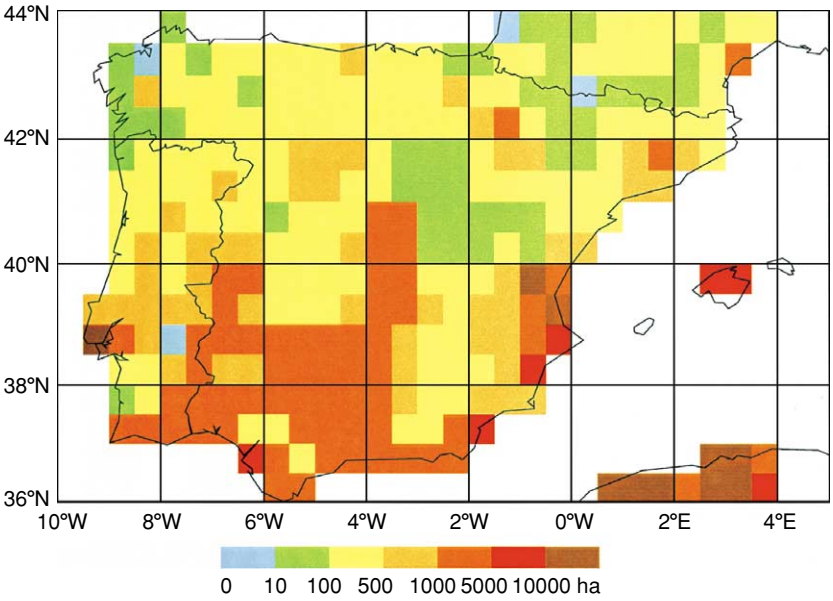

Fig. 3 Simulated areas burnt (ha) on the Iberian peninsula during 1974–94.

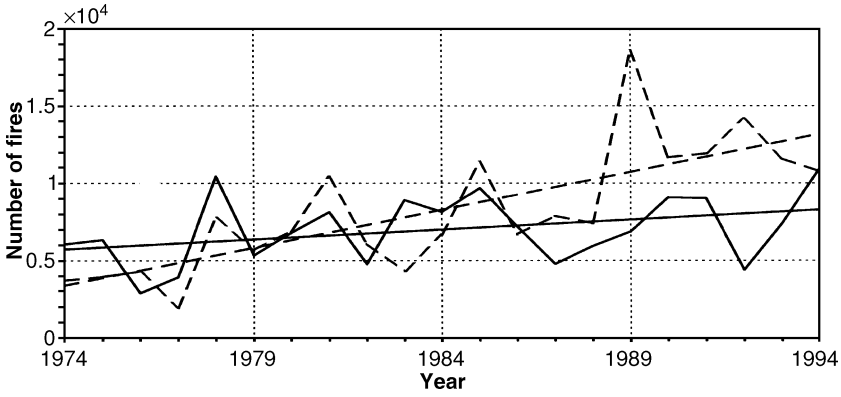

Fig. 4 Time series of the total number of fires in peninsular Spain during 1974–94. The dashed and solid lines represent the observed and simulated number of fires, respectively.

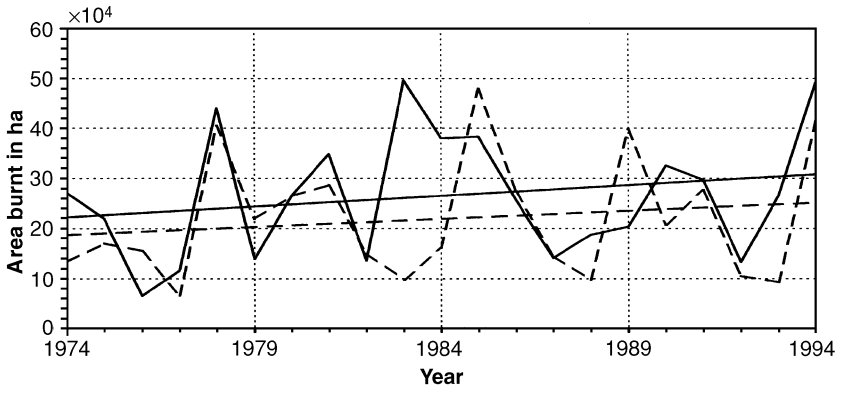

Fig. 5 Time series of the total area burnt (ha) in peninsular Spain during 1974–94. The dashed and solid lines represent the observed and simulated area burnt, respectively.

1998). A large area of peninsular Spain has between two and 20 fires per 10 000 ha and an area burnt between ten and 1000 ha for the two decades, which agree well with the fire statistics for the entire period (see Fig. 2).

The spatial distribution of number of fires fits observation better than the distribution of areas burnt, reflecting considerable differences in climate conditions and population concentration in different regions of the country. The largest number of fires over the 20 year period (50–100 fires per 10 000 ha) were both simulated and observed in the coastal zone of southern Spain in provinces of Andalusia, Valencia and Catalonia, as well as near big cities like Madrid and San Sebastian. The lowest number of fires (two to nine fires per 10 000 ha for 1974–94) were both simulated and observed for the Iberian mountain system, the Zaragoza province and the Pyrenees. The model underestimates the number of fires in the Galician province and in the Cantabrian Mountains (2–50 fires per 10 000 ha in 1974–94 against 50–100 observed fires). This underestimation is most likely related to the high number of intentional ignitions in the region initiated mainly in the early nineties (see Figs 5 and 12 in Moreno *et al*., 1998).

Both observed and simulated geographical distributions of areas burnt for 1974–94 are generally more smooth than for number of fires, e.g. in mountainous regions of Catalonia, Valencia and Andalusia (see Fig. 3). In the model, vegetation pattern influences fuel composition in these regions damping a rapid spread of fires. Again the largest areas burnt both observed and simulated (100–10 000 ha in 1974–94) occur in the coastal Mediterranean zone, while areas burnt are considerably less in the northeastern part of Spain (10–500 ha in 1974–94). The model does not reproduce large areas burnt in Galicia and the Cantabrian Mountains because the number of fires in these regions is underestimated.

Annual dynamics of fires in Spain for 1974–94

The observed total number of fires and areas burnt over peninsular Spain between 1974 and 1994 were extracted from Table 1 in Moreno *et al*. (1998) and compared against the simulated totals (see Figs 4 and 5).

It can be seen that observed and simulated number of fires and areas burnt have similar annual dynamics. The annual mean number of fires and areas burnt are well reproduced. The simulated number of fires has the same maximum-minimum sequence until 1988, except for 1983 (see Fig. 4). In 1983 the number of fires and areas burnt are simulated to increase (which is opposite to fire

statistics data) as a consequence of a considerable drop in monthly precipitation seen in the input climate data. The simulated and observed areas burnt generally have the same temporal pattern, except in 1983 and 1989–90 (see Fig. 5). In some years, the simulated number of fires exactly matches observation, while the corresponding annual area burnt is lower (compare year 1979 and 1980 in Figs 4 and 5). Here, simulated conditions for fire spread differ from those observed. Discrepancies in vegetation composition, indirectly influencing fire spread through specific fuel characteristics, and in simulated moisture conditions might have reduced fire spread and thus area burnt. A good correlation in temporal patterns between observed number of fires and areas burnt is obtained for peninsular Spain before 1989 (compare with Fig. 2 in Moreno *et al*., 1998). The discrepancy thereafter may be an indication of possible problems in the fire history records for these five years. Possible socio-economic changes in land use practices in this time accompanied with improvements in fire management and fire detection in Spain may be one of the explanations for the dramatic increase in number of fires while the increase in area burnt is lower (compare Figs 4 and 5). However, the formulation of human-caused ignitions in Reg-FIRM may not be sufficient to capture changes in fire causes as well as fire management after 1989.

The observed and simulated annual trend and amplitude of total areas burnt in Spain coincides well (see Fig. 5), while the simulated number of fires has both a smaller trend and amplitude than observed (Fig. 4). There are a few possible explanations for such model behaviour, e.g. soil moisture dynamics may not be simulated correctly by LPJ-DGVM, or the monthly averaging of fire danger index can produce a too rough approximation, compared with the daily fire danger index. However, the most likely reason is absence of dynamic land use changes in LPJ-DGVM for the simulated period. The socio-economic changes, which have taken place in the last decades in the southern EU countries, e.g. rural exodus and abandonment of agricultural lands, reduced grazing pressure, urbanization of some rural areas, are mentioned by many authors (Rego, 1992; Vélez, 1997; Moreno *et al*., 1998) as some of the main reasons of notable changes in the number of fires and areas burnt in these countries.

Dynamics of fires by size for the period 1974–94

The annual area distributions for peninsular Spain in terms of numbers of fires and the surface burned were calculated from Table 3 in Moreno *et al*. (1998) and compared with the simulated distributions for the period 1974–94. This table contains the number of 10×10 km grid cells for each case subdivided into five classes. For the comparison exercise we reclassified the data for both cases into two classes and summed areas, where no fires were observed. There were a total of 220 grid cells at 0.5° resolution for peninsular Spain, and therefore 5500 grid cells at a 10-km resolution (assuming each large cell contains 25 smaller ones). The two classes, from 0 to 3 fires per 100 km^2 (S – area with few ignitions) and more than 3 fires per 100 km^2 (F – area with frequent ignitions) were defined for the numbers of fires comparison. Similarly for the surface burned we defined two classes: grid cells having the surface burned less than 100 ha per 100 km^2 (A is the area with fires of average or small size) and more than 100 ha per 100 km^2 (L is the area with large fires). The observed distributions in 1974–94 for the four classes at the 10 km resolution (in fractions) are presented in Table 2.

For each year the 220 grid cells at 0.5° resolution were allocated into the four classes, according to the simulated numbers of fires and the simulated surface burned. The total number of cells in the two larger classes (S-grid cells with less than three ignitions per 100 km^2 and A-grid cells, having less than 100 ha burned per 100 km^2) was compared against observation, obtained by multiplying 220 by the ratios from Table 2. The two larger classes (S and A) were taken for comparison with observations in order to investigate the model's ability to capture major features of fire patterns in Spain. Besides, the two smaller classes (F-area with frequent ignitions and L area with large fires) have a complementary dynamics.

The observed and simulated total numbers of grid cells in the two classes have similar temporal dynamics, although the magnitude differs slightly. The calculated mean number of grid cells for the class S in the period 1974–94 is 207 compared with 191 observed, while the calculated mean number of grid cells for the class A in the same period is 192 compared with 206 observed. Such discrepancy follows from the comparison method of two samples with significantly different sizes (5500 and 220) due to loss of information during sample aggregation. Indeed, the inner heterogeneity of the grid cells at 10 km resolution within the larger 0.5° cells can considerably affect the final distributions in the four classes. Spatial dependency in statistical geo-referenced data analysis (so-called *modifiable area unit problem*) is well recognized, but the problem has still not been resolved (Wong, 1996). In our case, to avoid the systematic bias of the method we subtracted the means of the two classes from observed and simulated time series and compared the dynamics of anomalies. (see Figs 6 and 7)

The dynamics of anomalies for areas with few ignitions and for areas with fires of small or average size are simulated rather realistically. We have inversions for simulated dynamics of anomalies for the number of grid cells in the class S in only four years (1976, 1983,

Table 2 Distributions of 10 km resolution grid cells for four classes in peninsular Spain during the period 1974–94 (fractions to the total)

Year	0–3 fires per 100 km^2 (S)	> 3 fires per 100 km^2 (F)	Surface burned < 100 ha per 100 km^2 (A)	Surface burned > 100 ha per 100 km^2 (L)
1974	0.925	0.075	0.948	0.052
1975	0.937	0.063	0.952	0.048
1976	0.920	0.080	0.946	0.054
1977	0.959	0.041	0.976	0.024
1978	0.865	0.135	0.896	0.104
1979	0.909	0.091	0.935	0.065
1980	0.862	0.138	0.907	0.093
1981	0.838	0.162	0.902	0.098
1982	0.884	0.116	0.940	0.060
1983	0.907	0.093	0.968	0.032
1984	0.883	0.117	0.939	0.061
1985	0.815	0.185	0.866	0.134
1986	0.872	0.128	0.922	0.078
1987	0.873	0.127	0.942	0.058
1988	0.866	0.134	0.952	0.048
1989	0.779	0.221	0.881	0.119
1990	0.813	0.187	0.927	0.073
1991	0.815	0.185	0.928	0.072
1992	0.831	0.169	0.958	0.042
1993	0.852	0.148	0.975	0.025
1994	0.841	0.159	0.956	0.044

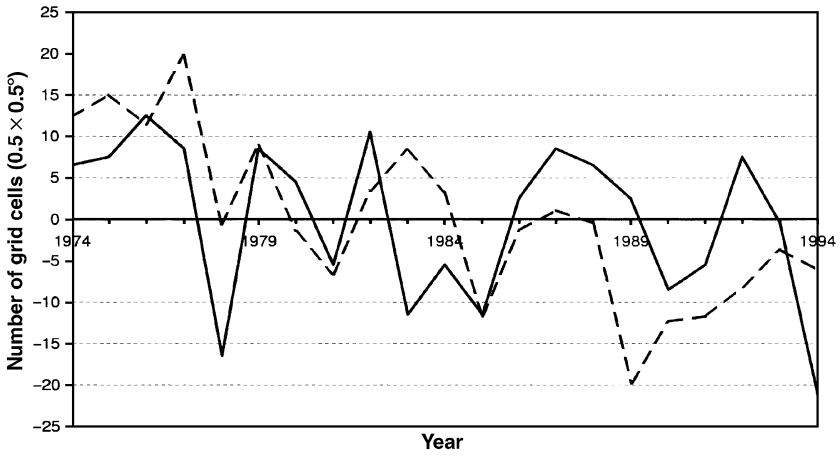

Fig. 6 Area anomalies for fires less than 3 per 100 km^2 in 1974–94 (units are number of grid cells $0.5 \times 0.5°$). The dashed and solid lines represent the observed and simulated area anomalies, respectively.

1989, 1993) and a large difference in the magnitudes in 1994. The additional inversion in 1988 appears for simulated dynamics of anomalies for the number of grid cells in the class A, thus the application of the fire spread model does not result in considerable, additional error. The temporal patterns of areas with few ignitions and for areas with fires of small or average size are well reproduced in all other years. Therefore the model is able to reproduce major features of annual dynamics for geographical patterns of ignitions and fire regimes, although more accurate spatial statistical analysis is needed if observed geo-referenced data is available.

However, the simulated time series have larger amplitude than those observed (especially in the case for anomalies of areas with fires of small or average size). Most likely only a simulation on a daily (not on monthly) time step can produce a closer fit for these time series, because the fire danger index and the spread of fire are sensitive to precipitation and the wind speed.

Discussion

This study can be considered a successful application of a relatively simple mechanistic fire model in reproducing

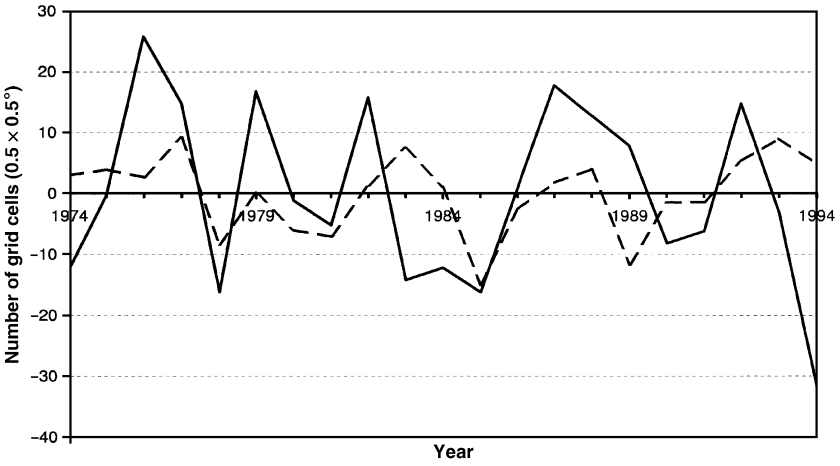

Fig. 7 Area anomalies for less than 100 ha burned per 100 km^2 in 1974–94 (units are number of grid cells 0.5 × 0.5°). The dashed and solid lines represent the observed and simulated area anomalies, respectively.

both spatial and temporal dynamics of fire over a large region and a long time period. By making simple assumptions about climate and human-induced changes, the fire model allows investigation of fire regimes on different time scales over large geographical regions. Processes selected to describe fire at the regional scale are at the right level of explicitness as the agreement in the temporal patterns demonstrates. Simulation results at a monthly resolution show that it is possible to study fire-vegetation feedbacks using a mechanistic approach instead of stochastic modelling of fires that require more computer resources and parameter values.

The relatively good agreement between observed and simulated number of fires demonstrates the importance of both the climatic fire risk and the ignition sources, on fire occurrence (see Fig. 4). The reproduced pattern shows the impact of inter-annual climate variability on fire, since in this simulation study we assumed a constant number of ignitions per human, expressed in a constant a(N_d) (see equation 10). By keeping both wind speed and fire duration constant one can isolate the individual impact of vegetation (see equations 16, 17 and 20). Since a good agreement between simulated and observed area burnt was obtained this implies that vegetation has a dominant influence on fire. Fires cannot spread if the fuel bed is too moist or the amount of fuel is too low, despite multiple ignitions. However, in the case of large, convective fires this influence is neglected due to extremely high fire intensities. Consideration of convective fires, as an extreme fire event, lies beyond the focus of Reg-FIRM. Therefore, the generalizations made here to describe fire spread, and thus area burnt, at the regional scale are sufficient to reproduce the observed pattern.

The constant value for human-caused ignitions taken here seems to adequately represent a country-wide aggregate of all different regional motivations for humans to set fire in peninsular Spain (see Fig. 4). There are different factors, which could contribute to improve the simulated spatial patterns of both, number of fires and area burnt, since inconsistencies in simulated number of fires drive the final area burnt per grid cell (see equation 1). The assumption that different life styles in rural and urban areas can be assigned to a certain population density, is very likely valid in only a few regions of peninsular Spain. A regionally specific formulation of a(*Nd*) (see equation 10), describing regionally different land management systems in terms of their motivations to set fire especially in rural areas, could improve the simulation results. Another potential improvement would be the explicit consideration of land use and its changes in Reg-FIRM, or LPJ-DGVM as a whole.

This would reduce the potential area burnt in grid cells, where land use types such as settlement areas and permanent agriculture reduce the size of unmanaged land. A sharpening of the hitherto smooth spatial distributions of simulated area burnt would result (see Fig. 5), whilst not affecting the validity of the model concept.

In addition, inclusion of land cover and land use changes would lead to an increase in simulated number of fires and area burnt in regions, where potential area burnt increased in recent years due to the effects of land abandonment (re-vegetation and fuel build-up and therefore higher connectivity of the fuel bed), and where fire causes changed concurrently, e.g. shift from setting fire for pasture improvement to negligence due to tourist activities (see Pausas & Vallejo, 1999). This might contribute to improve the model performance in the northwest of Spain.

In-depth studies should investigate the impact of these factors on the Iberian fire regime, to get a further insight into the interactions and feedbacks between fire regime, land use and vegetation composition.

Another possible improvement would be to implement an explicit lightning-ignition model, recognizing

lightning-caused ignition as a function of elevation, thus improving the results in mountainous regions. A re-parameterization is required if Reg-FIRM were to be applied to new study areas, e.g. the values of lightning and human-caused ignitions, wind speed and fire duration must be changed. Implementation of a lightning-ignition model, however, would enhance the applicability of Reg-FIRM to other study areas, where for example the ratio between lightning and human-caused ignitions is higher.

Reg-FIRM can be incorporated in any dynamic vegetation model (DVM), given the DVM can provide the necessary input to drive the fire model. It can be used to investigate both the causes and effects of fire on vegetation and the long-term feedbacks of vegetation on the fire regime. One example is the simulation study presented here. The advantage of this model concept is that the model can be calibrated and the results validated using the type of data, which are usually collected in official fire statistics, such as fire danger, number of fires and area burnt. As was the aim of this study, it has been shown that human-caused fires can be included in regional-scale fire modelling using a mechanistic approach, and both climatic and human ignition potentials are needed to describe observed pattern sufficiently. The relative impacts of climate variability and human population development on fire dynamics can be assessed by sensitivity analysis within Reg-FIRM for representative regions, providing insight into socio-economic and biophysical components of global change. Therefore, Reg-FIRM can be seen as a useful tool to study the development of fire regime and vegetation under future global change conditions.

References

Albini FA (1976) *Estimating Wildfire Behaviour and Effects.* Intermountain Forest and Range Experiment Station. Forest Service. U.S. Department of Agriculture, USDA. Forest Service General Technical Report INT-30.

Barbosa PM, Stroppiana D, Grégoire JM *et al.* (1999) An assessment of vegetation fire in Africa (1981–91): Burned areas, burned biomass, and atmospheric emissions. *Global Biogeochemical Cycles*, **13** (4), 933–950.

Davis FW, Burrows DA (1994) Spatial Simulation of Fire Regimes in Mediterranean-Climate Landscapes. In: *The Role of Fire in Mediterranean-Type Ecosystems* (eds Moreno JM, Oechel W), pp. 117–139. Springer Verlag, Berlin.

Davis KP, Byram GM, Krumm WR (1959) *Forest Fires: Control and Use*. McGraw-Hill, New York.

Deeming JE, Lancaster JW, Fosberg MA *et al.* (1974) *The National Fire-Danger Rating System*. US Department of Agriculture. Research paper no. RM-84.

Demidov PG, Saushev VS (1975) *Gorenie I Svoistva Goriuchich Materialov* Nauka, Moscow.

Enting IG, Wigley TML, Heimann M (1994) Future emissions and concentrations of carbon dioxide: Key ocean/atmosphere/land analyses. CSIRO Division of Atmospheric Research. 31.

FAO (1991) *The Digitized Soil Map of the World (Release 1.0).* Food and Agriculture Organization of the United Nations. 67/1.

Far Eastern Forest Institute (1987) *Rekomendazii po bor'be s krupnymi lesnymi pozharami na Dal'nem Vostoke*. Far Eastern. Forest Institute.

Finney MA (1994) Modelling the spread and behaviour of prescribed natural fires. In: (*12th Conference on Fire and Forest Meteorology*) (pp. 138–144.). Bethesda, MD: Soc. of Am. For.

Gardner RH, Romme WH, Turner MG (1999) Predicting Forest Fire Effects at Landscape Scales. In: *Spatial Modelling of Forest Landscapes: Approaches and Applications* (eds Mladenoff DJ, Baker WL), pp. 163–185. Cambridge University Press, Cambridge.

Goldammer JG, Jenkins MJ (1990) *Fire in Ecosystem Dynamics: Mediterranean and Northern Perspectives* SPB. Academic Publishers, The Hague.

Haxeltine A, Prentice IC (1996) A general model for the light-use efficiency of primary production. *Functional Ecology*, **10**, 551–561.

Hulme M (1995) *A Historical Monthly Precipitation Dataset for Global Land Areas from 1990 to 1997, Gridded at 3.75 X 25 Resolution Climate Research Unit*. University of East Anglia.

Instituto Nacional de Estadística (1999) *TEMPUS database*. Instituto Nacional de Estadística.

IPCC (1995) *Climate Change 1995–the Science of Climate Change*. Contribution of Working Group I to the second assessment report of the Intergovernmental Panel on Climate Change. Cambridge University Press, Cambridge, UK.

Johnson EA, Gutsell SL (1994) Fire Frequency Models, Methods and Interpretations. *Advances in Ecological Research*, **25**, 239–287.

Jones PD (1994) Hemispheric surface air temperature variations: a reanalysis and an update to 1993. *Journal of Climate*, **7**, 1794–1802.

Keane RE, Long DG (1998) A Comparison of Coarse Scale Fire Effects Simulation Strategies. *Northwest Science*, **72** (2), 79–90.

Keane RE, Long DG, Menakis JP *et al.* (1996a) *Simulating Coarse-Scale Vegetation Dynamics Using the Columbia River Basin Succession Model-CRBSUM* USDA. Forest Service Intermountain Research Station, Ogden, Utah. Research paper no. INT-GTR-340.

Keane RE, Morgan P, Running SW (1996b) FIRE-BGC – A Mechanistic Ecological Process Model for Simulating Fire Succession on Coniferous Forest Landscapes of the Northern Rocky Mountains. *USDA*. Forest Service Intermountain Research Station. Research Paper INT-RP-484.

Korovin GN (1996) Analysis of the Distribution of Forest Fires in Russia. In: *Fire in Ecosystems of Boreal Eurasia* (eds Goldammer JG, Furyaev VV), pp. 112–128. Kluwer. Academic Publishers, Dordrecht, Boston, London.

Lenihan JM, Neilson RP (1998) Simulating Broad-Scale Fire Severity in a Dynamic Global Vegetation Model. *Northwest Science*, **72** (1998), 91–103.

Levine JS, (ed.) (1996) *Biomass Burning and Global Change*. The MIT Press, Cambridge, Massachusetts, London, England.

McKenzie D, Peterson DL, Ernesto A (1996) Extrapolation problems in modelling fire effects at large scales. *International Journal of Wildland Fire*, **6** (4), 165–176.

Melekhov IS (1978) *Lesnaia Pirologia*. Lesnaia promyshlennost', Moskow.

Merida J-C (1999) Descripción de los modelos combustibles usados en la prediccion del comportamiento del fuego. *Àrea de Defensa Contra Incendios Forestales*. Ministerio de Medio Ambiente España.

Moreno JM, Vázquez A, Vélez R (1998) Recent History of Forest Fires in Spain. In: *Large Forest Fires* (ed. Moreno JM), pp. 159–185. Backhuys Publishers, Leiden.

Moritz MA (1997) Analysing Extreme Disturbance Events: Fire in Los Padres National Forest. *Ecological Applications*, **7** (4), 1252–1262.

Ndambiri JK, Kahuki CD (2001) Fire situation in Kenya. *International Forest Fire News*, **25**, 12–14.

Nesterov VG (1949) *Gorimost' lesa i metody eio opredelenia*. Goslesbumaga Moscow.

Pausas JG, Vallejo R (1999) The role of fire in European Mediterranean ecosystems. In: *Remote Sensing of Large Wildfires in the European Mediterranean Basin* (ed. Chuvieco E), pp. 3–16. Springer Verlag, Berlin Heidelberg.

Rego FC (1992) Land use changes and wildfires. In: *Responce of Forest Ecosystems to Environmental Changes* (eds Teller, Mathy P, Jeffers JNR), pp. 367–373. Elsevier, London.

Rothermel RC (1972) *A Mathematical Model for Predicting Fire Spread in Wildland Fuels.* Intermountain Forest and Range Experiment Station. Forest Service. U.S. Department of Agriculture, USDA. Forest Service General Technical Report INT-115.

Running SW, Nemani RR, Hungerford RD (1987) Extrapolation of synoptic meteorological data in mountainous terrain and its use for simulating forest evapotranspiration and photosynthesis. *Canadian Journal of Forest Research*, **17**, 472–483.

Shvidenko A, Nilsson S, Stolbovoi V *et al.* (1998) *Background information for carbon analysis of Russian forest sector*. IIASA.

Sitch S, Smith B, Prentice IC *et al.* (2002) Evaluation of ecosystem dynamics, plant geography and terrestrial carbon cycling in the LPJ Dynamic Global Vegetation Model. *Global Change Biology* (in press).

Stocks BJ (1991) The Extent and Impact of Forest Fires in Northern Circumpolar Countries. In: *Global Biomass Burning: Atmospheric, Climatic, and Biospheric Implications* (ed. Levine JS), pp. 197–202. The. MIT Press, Cambridge, Massachusetts; London, England.

Stocks BJ, Cahoon DR, Levine JS *et al.* (1996) Major 1992 forest fires in Central and Eastern Siberia: Satellite and Fire Danger Measurements. In: *Fire in Ecosystems of Boreal Eurasia* (eds Goldammer JG, Furyaev VV), pp. 139–150. Kluwer. Academic Publishers, Dordrecht, Boston, London.

Telitsyn HP (1996) A Mathematical Model of Spread of High-Intensity Forest Fires. In: *Fire in Ecosystems of Boreal Eurasia* (eds Goldammer JG, Furyaev VV), pp. 139–150. Kluwer. Academic Publishers, Dordrecht, Boston, London.

Telitsyn (1988) *Lesnye Pozhary, Ich Preduprezhdenie I Bor'ba S Nimi V Khabarovskom Krae* DALNIILKH, Khabarovsk.

Thomas PH (1965) The contribution of flame radiation to fire spread in forests. Joint Fire Research Organization. 594.

Thonicke K, Venevski S, Sitch S *et al.* (2001) The role of fire disturbance for global vegetation dynamics: coupling fire into a Dynamic Global Vegetation Model. *Global Ecology and Biogeography*, **10** (6), 661–678.

Valendik EN, Matveev PM, Sofronof MA (1978) *Krupnye Lesnye Pozhary* Nauka, Moscow.

Van Wagner CE (1969) A simple-fire growth model. *Forestry Chronicles*, **45** (2), 103–104.

Van Wagner CE (1987) *Development and Structure of the Canadian Forest Fire Weather Index System*, Canadian Forestry Service, Forest Technical Report 35.

Vázquez A, Moreno JM (1998) Patterns of Lightning-, and People-Caused Fires in Peninsular Spain. *International Journal of Wildland Fire*, **8** (2), 103–115.

Vélez R (1997) Recent history of forest fires in Mediterranean area. In: *Forest Fire Risk and Management* (ed. Commission E), pp. 15–28. Office for official publication of the European Community, L-2985 Luxembourg.

Whelan RJ (1995) *The Ecology of Fire*. Cambridge University Press, Cambridge.

Wong D (1996) Aggregation Effects in geo-referenced data. In: *Practical Handbook of Spatial Statistics* (ed. Arlinghaus SL), pp. 83–106. CRC Press, Boca Raton, Florida.

Zobler L (1986) *A World Soil File for Global Climate Modelling*. Goddard Institute for Space Studies.